Dynamic Behavior of Cracked Flexible Rotor Subjected to Constant Driving Torque

Jerzy T. Sawicki
Rotor-Bearing Dynamics & Diagnostics Laboratory, Fenn College of Engineering
Cleveland State University, Cleveland, OH 44115, U.S.A.

Xi Wu
Rotor-Bearing Dynamics & Diagnostics Laboratory, Fenn College of Engineering
Cleveland State University, Cleveland, OH 44115, U.S.A.

George Y. Baaklini
NASA Glenn Research Center, 21000 Brookpark Road, MS 6-1, Cleveland, OH 44135

Michael I. Friswell
University of Bristol, Department of Aerospace Engineering, Bristol BS8 1TR, UK

ABSTRACT

The dynamic behavior of a cracked flexible rotor passing through critical speed under the presence of a constant driving torque is analyzed. By incorporating the nonlinear coupling between the bending and torsional degrees of freedom, the model more accurately describes the behavior of the accelerated cracked rotor, especially near the resonance. The breathing types of cracks are considered using simple hinge model for small cracks and cosine function for deep ones. The applied strategy enables to study the cracked rotor dynamic response with and without weight dominance, taking into account also nonsynchronous whirl. The local cross-flexibility for deep cracks is taken into account. The effect of crack on "stalling" of the rotor is investigated. Under the constant driving torque, the vibration amplitude increases and the stalling angular velocity decreases with the depth of the crack.

Keywords: Rotor, crack, acceleration, torque, stalling.

1. INTRODUCTION

In many cases the rotors of modern machines are rapidly accelerated from rest to operating speed to reduce the excessive vibrations at the critical speeds. Also, the vibration monitoring during startup or shutdown has been receiving growing attention, especially for machines such as aircraft engines, which are subjected to frequent starts and stops as well as high speeds and acceleration rates [1]. It has been recognized that the

presence of angular acceleration strongly affects the rotor's maximum response to unbalance and the speed at which it occurs.

The topic of transient cracked rotor response has been treated by number of published works [2-4]. They have been focused on the study of dynamic behavior of rotor with the so-called breathing type of crack during the passage through a critical speed at constant angular acceleration or deceleration. Sekhar [2-3] investigated the transient vibration response of a cracked rotor passing its critical speed, utilizing a simple hinge model for small cracks. He followed an assumption that the vibrations remain small in comparison to the rotor's sag. If a cracked shaft rotates under the load of its weight, then the crack will open and close once per revolution, in a case of synchronous whirl. Sawicki et al. [4] studied accelerating cracked rotor response using the angle between the crack centerline and the rotor whirl vector to determine the closing and opening of the crack, which allows to study the rotor dynamic response with and without the rotor weight dominance by taking into account also nonsynchronous whirl.

Few authors [5-7] studied the dynamic response of the uncracked rotors subjected to constant driving torque. Markert et al. [5] determined the maximum deflection of a Jeffcot rotor during the acceleration through the critical speed or during stalling in resonance as function of the three nondimensional system parameters, i.e., damping ratio, eccentricity ratio and driving torque. Later, Gasch et al. [6] applied these strategies to a practical flexible rotor with a continuous mass distribution passing through its critical speeds under a constant driving torque. Genta and Delprete [7] developed a mathematical finite element–based model to study the nonlinear behavior of complex anisotropic rotors with non-constant angular speed.

There is a wealth of published research results on cracked rotors. Wauer [8] and Dimarogonas [9] provided a comprehensive literature reviews and state-of-the-art of vibration of cracked structures. Gasch [10] provided a comprehensive investigation of the stability behavior of a cracked Jeffcott rotor and the forced vibration due to unbalance and crack with a constant spinning speed. Penny and Friswell [11] demonstrated the influence of the crack model on the response of Jeffcott rotor.

In this paper the effect of breathing crack on the unbalance response of the accelerating rotor subjected to constant driving torque is studied. The equations for lateral rotor's motion are supplemented by additional equation relating the angular displacement and the driving torque. Torsional elasticity of the shaft is neglected due to the assumption that the torque is applied to torsionally stiff rotor. The effect of crack on stalled rotor's angular velocity and maximum amplitude of unbalance response is presented.

2. CRACK MODELS AND STIFFNESS MATRIX

The theoretical model, called the *Jeffcott rotor*, employs a flexible rotor composed of a centrally located unbalanced disk attached to a massless elastic shaft which is, in turn, mounted symmetrically on rigid bearings (see Fig. 1(a). The shaft does have a transverse crack running across its section and located close to the disk. The stiffness of the uncracked rotor system is symmetric (isotropic) and the damping due to the air resistance effect is assumed to be viscous. The rotor is driven by a constant external drive torque. The angle between the crack centerline and the line connecting the bearings and shaft

center (Fig. 1(b)), $y = \Phi - \arctan(y/z)$, is used to determine the closing and opening of the crack. At any instant of time, the x-axis remains perpendicular to the face of the crack, causing that the body-fixed rotating coordinate frame (z,h,x) rotates with the same velocity as the rotor. The weight dominance assumed in almost all previous analyses of horizontal cracked rotors is not required, and the influence of the whirl speed on the closing and opening of crack is included. This nonlinear system with time-varying stiffness coefficients is studied numerically, with particular focus on the effect of different crack depths on the rotor stalling.

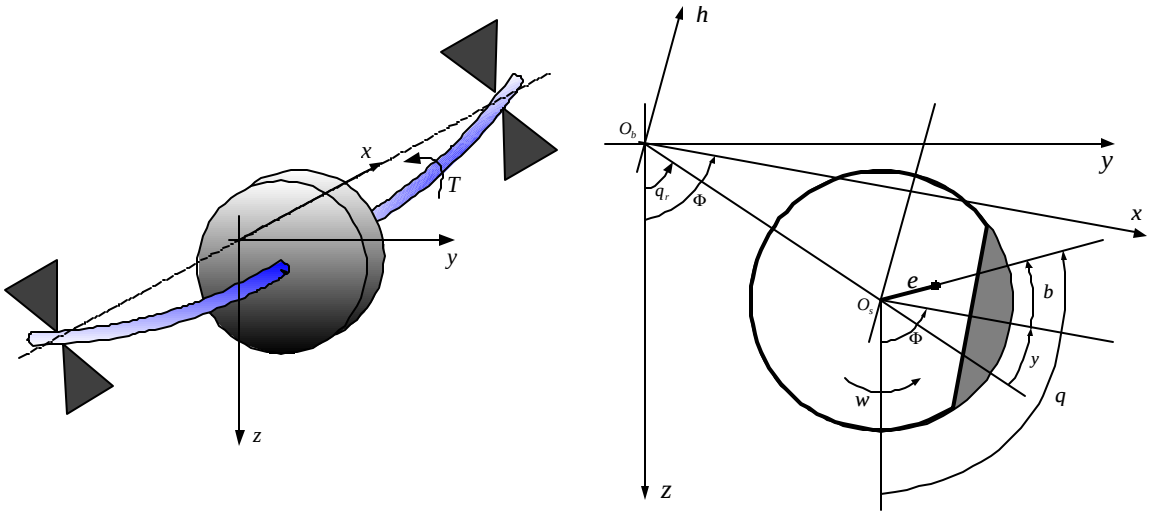

(a) **(b)**

Fig. 1 Model of Jeffcott rotor with crack and constant driving torque (a), crack section in inertial and rotating coordinates (b).

The stiffness matrix for a Jeffcott rotor with a cracked shaft in rotating coordinates can be written as:

$$\mathbf{K}_R = \begin{pmatrix} K & 0 \\ 0 & K \end{pmatrix} - f(y) \begin{pmatrix} \Delta k_x & 0 \\ 0 & \Delta k_h \end{pmatrix} \tag{1}$$

where the first matrix refers to the stiffness of the uncracked shaft, and the second defines the changes in stiffness Δk_x and Δk_h in x and h directions, respectively. The function $f(y)$ is a crack steering function which depends on the angular position of the crack y and the selected crack model.

The simplest model of crack is a hinge model, where the crack is assumed to change from its closed to open state suddenly as the shaft rotates. The steering function for this model is defined as

$$f(y) = \begin{cases} 0 & \text{for} \quad x < 0 \\ 1 & \text{for} \quad x \geq 0 \end{cases} \tag{2}$$

or, using Fourier expansion is

$$f(y) = \frac{1}{2} + \frac{2}{p}\cos y - \frac{2}{3p}\cos 3y + \frac{2}{5p}\cos 5y - \ldots \tag{2a}$$

While the hinge model might be proper representation for very small cracks Mayes and Davies [12-13] proposed a model with a smooth transition between the opening and closing of the crack, which is more adequate for bigger cracks. In this case the crack steering function or the Mayes modified function takes the following form:

$$f(y) = \frac{1+\cos(y)}{2} \tag{3}$$

Now, the stiffness matrix for a Jeffcott rotor with a cracked shaft in inertial coordinates, $\mathbf{K}_I$ is given by

$$\mathbf{K}_I = \mathbf{T}\mathbf{K}_R\mathbf{T}^{-1} \tag{4}$$

where the transformation matrix $\mathbf{T}$ is

$$\mathbf{T} = \begin{pmatrix} \cos\Phi & -\sin\Phi \\ \sin\Phi & \cos\Phi \end{pmatrix} \tag{5}$$

Thus

$$\mathbf{K}_I = \mathbf{T}\mathbf{K}_R\mathbf{T}^{-1} = \begin{pmatrix} K & 0 \\ 0 & K \end{pmatrix} - \frac{f(y)K}{2}\begin{pmatrix} \Delta k_1 + \Delta k_2\cos 2\Phi & \Delta k_2 \sin 2\Phi \\ \Delta k_2 \sin 2\Phi & \Delta k_1 - \Delta k_2 \cos 2\Phi \end{pmatrix} \tag{6}$$

where $\Delta k_1 = \dfrac{\Delta k_x + \Delta k_h}{K}$ and $\Delta k_2 = \dfrac{\Delta k_x - \Delta k_h}{K}$.

3. EQUATIONS OF MOTION OF CRACKED ROTOR UNDER CONSTANT DRIVING TORQUE

The nonlinear coupled equations of motion for the accelerating Jeffcott rotor with a cracked shaft, subjected to constant driving torque, T_a, unbalance force, and gravitational force due to its weight, can be written in inertial coordinate frame as:

$$\mathbf{M}\ddot{\mathbf{q}} + \mathbf{C}\dot{\mathbf{q}} + \mathbf{K}_I\mathbf{q} = \begin{pmatrix} Me\left(\dot{\Phi}^2\cos q + \ddot{\Phi}\sin q\right) \\ Me\left(\dot{\Phi}^2\sin q - \ddot{\Phi}\cos q\right) \end{pmatrix} + \begin{pmatrix} Mg \\ 0 \end{pmatrix} \tag{7.1}$$

$$\left(J_p + Me^2\right)\ddot{q} + Me\left(-\ddot{z}\sin q + \ddot{y}\cos q\right) = T_a \tag{7.2}$$

where $\mathbf{M}=\begin{pmatrix} M & 0 \\ 0 & M \end{pmatrix}$ and $\mathbf{C}=\begin{pmatrix} C & 0 \\ 0 & C \end{pmatrix}$ is the rotor mass and damping matrix, respectively, $\mathbf{q}=\begin{pmatrix} z & y \end{pmatrix}^T$ is the vector of the disk's displacements, and Φ is the rotor spin angle (see Fig. 1(b)).

Using Eq. (7.1) one can eliminate lateral acceleration terms $\ddot{z}$ and $\ddot{y}$ from Eq. (7.2) to obtain the following form of the equation relating torque and the angular displacement:

$$J_p\ddot{\Phi}=T_a+eMg\sin q+eK\left(y\cos q-z\sin q\right)+eC\left(\dot{y}\cos q-\dot{z}\sin q\right)+\frac{ef(y)K}{2}\times$$
$$\left[\left(\Delta k_2\sin 2\Phi\right)\left(y\sin q-z\cos q\right)+\left(\Delta k_1+\Delta k_2\cos 2\Phi\right)z\sin q-\left(\Delta k_1-\Delta k_2\cos 2\Phi\right)y\cos q\right] \tag{7.3}$$

where $q=\Phi-b$, $y=\Phi-\arctan\left(\frac{y}{z}\right)$, $\dot{q}=\dot{\Phi}$, $\ddot{q}=\ddot{\Phi}$, and $J_p=Mr^2$.

Normalizing displacements with respect to unbalance eccentricity, introducing nondimensional time, damping, and torque, the equations (7.1) and (7.3) take the following nondimensional form:

$$\begin{pmatrix} 1 & 0 \\ 0 & 1 \end{pmatrix}\begin{pmatrix} Z'' \\ Y'' \end{pmatrix}+\begin{pmatrix} 2V & 0 \\ 0 & 2V \end{pmatrix}\begin{pmatrix} Z' \\ Y' \end{pmatrix}+\left\{\begin{pmatrix} 1 & 0 \\ 0 & 1 \end{pmatrix}-\frac{f(y)}{2}\begin{pmatrix} \Delta k_1+\Delta k_2\cos 2\Phi & \Delta k_2\sin 2\Phi \\ \Delta k_2\sin 2\Phi & \Delta k_1-\Delta k_2\cos 2\Phi \end{pmatrix}\right\}\begin{pmatrix} Z \\ Y \end{pmatrix}$$
$$=\begin{pmatrix} \Phi'^2\cos q+\Phi''\sin q \\ \Phi'^2\sin q-\Phi''\cos q \end{pmatrix}+\begin{pmatrix} \frac{g}{ew_n^2} \\ 0 \end{pmatrix} \tag{8.1}$$

$$\Phi''=T+\left(\frac{e}{r}\right)^2\left(Y\cos q-Z\sin q\right)+2V\left(\frac{e}{r}\right)^2\left(Y'\cos q-Z'\sin q\right)+\left(\frac{e}{r}\right)^2\frac{f(y)}{2}\left(\Delta k_2\sin 2\Phi\right)\times$$
$$\left(Y\sin q-Z\cos q\right)+\left(\frac{e}{r}\right)^2\left(\frac{f(y)}{2}\left(\Delta k_1+\Delta k_2\cos 2\Phi\right)Z\sin q+\frac{g}{ew_n^2}\sin q\right.$$
$$\left.-\frac{f(y)}{2}\left(\Delta k_1-\Delta k_2\cos 2\Phi\right)Y\cos q\right) \tag{8.2}$$

where the following definitions for nondimensional variables were employed:

$$Z=\frac{z}{e},\quad Y=\frac{y}{e},\quad t=w_nt,\quad w_n=\sqrt{\frac{K}{M}},\quad V=\frac{C}{2Mw_n},\quad T=\frac{T_a}{J_pw_n^2}$$
$$\Delta K=\frac{\Delta k_x}{K},\quad \left(\cdot\right)'=\frac{d(\cdot)}{dt}=\frac{1}{w_n}\frac{d(\cdot)}{dt},\quad \left(\cdot\right)''=\frac{d^2(\cdot)}{dt^2}=\frac{1}{w_n^2}\frac{d^2(\cdot)}{dt^2} \tag{8.3}$$

4. RESULTS AND DISCUSSION

Five nondimensional parameters have been used in the numerical study of accelerated cracked rotor, *i.e.*, T, $(e/r)^2$, ΔK, V, and $\frac{g}{ew_n^2}$. All following results were generated for the case where unbalance is in the direction of crack, i.e., $b = 0$. Also, the cross-stiffness for deep cracks has been accounted for as $\Delta k_h = \frac{\Delta k_x}{6}$ [13].

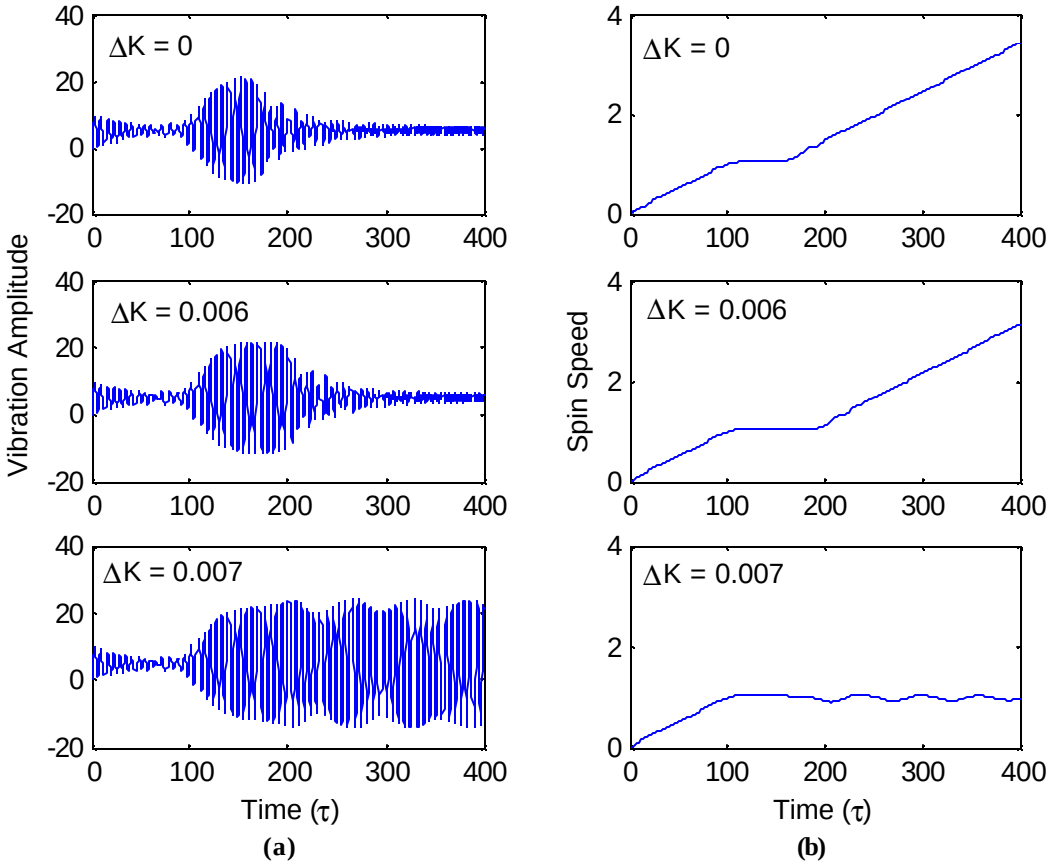

Fig. 2. Normalized vibration amplitude (a) and normalized spin speed (b) as a function of time; $T = 0.01$, $V = 0.02$, $(e/r)^2 = 0.85 \times 10^{-3}$, and $g/(ew_n^2) = 5$.

Figure 2 illustrates the behavior of the rotor passing through the critical speed for the uncracked and cracked rotor under the constant driving torque $T = 0.01$. The normalized rotor vibration amplitude and normalized spin speed are shown as a function of nondimensional time. It can be noticed that the appearance of the crack makes the zone of critical speed wider. Next, the slight increase of the depth of the crack, here by 0.001, causes that the rotor falls into the stalled condition, i.e., it fails to accelerate beyond the critical speed. In other words, all the power delivered by the given torque is dissipated by nonrotating damping [7] and the rotor acceleration is no longer possible.

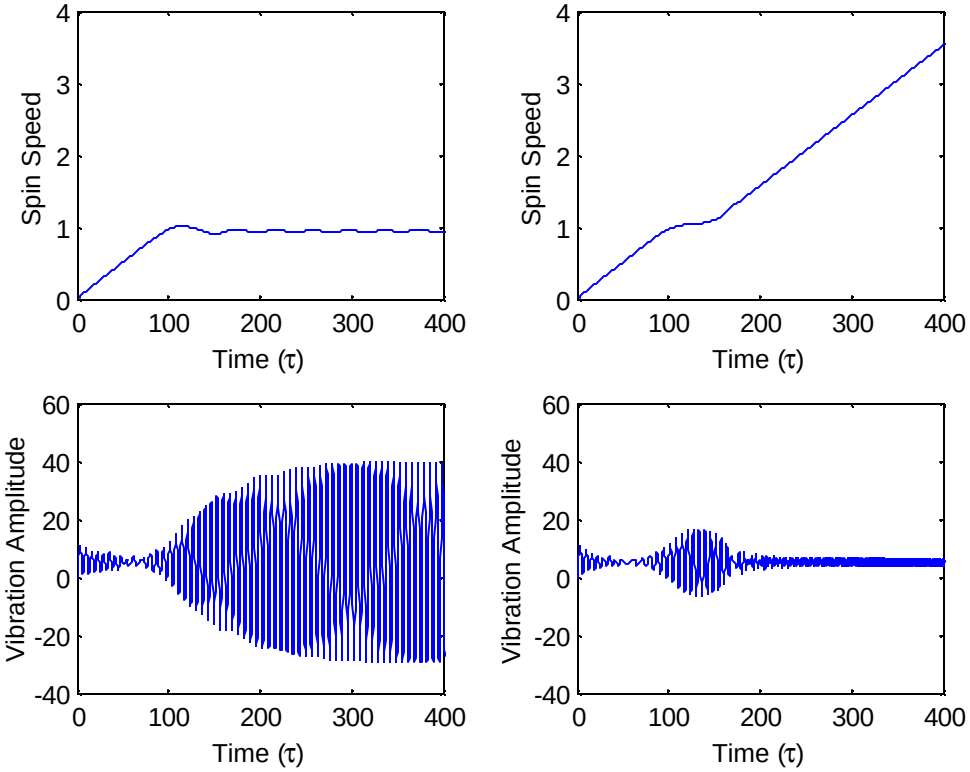

Fig. 3. Normalized shaft deflection and spin speed as a function of time for V = 0.02 (a), V = 0.04 (b); ΔK_x = 0.1, T =0.01, $(e/r)^2$ = 0.85 ´ 10^{-3}, $g/(ew_n^2)$ = 5 .

The effect of damping is illustrated in Fig. 3. The increased damping suppresses the stalling mechanism and the rotor can traverse through the critical speed.

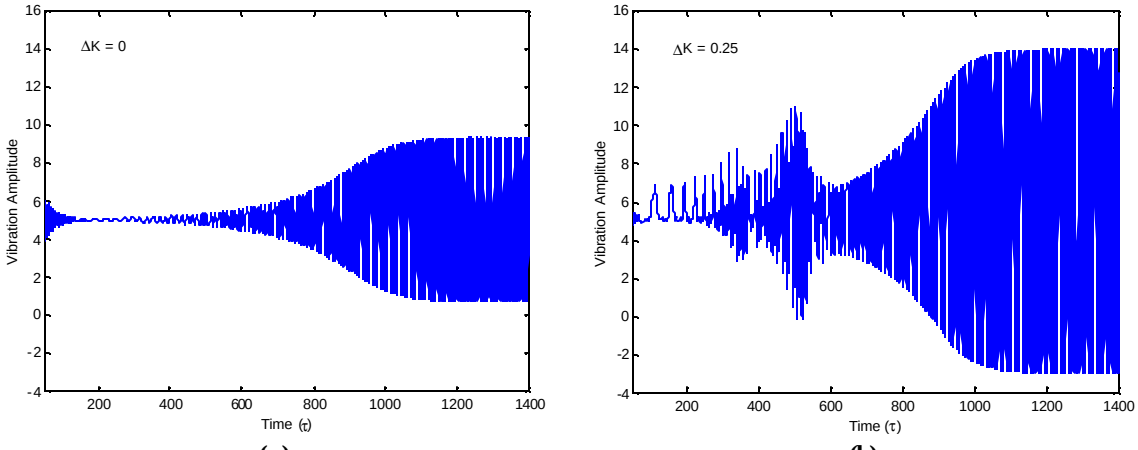

Fig. 4. Time history of normalized vibration amplitude for uncracked rotor (a) and with crack ΔK = 0.25 (b) at the stalled condition; V = 0.03, T =0.001, $(e/r)^2$ = 0.001, $g/(ew_n^2)$ = 5 .

Figure 4 illustrates that the appearance of crack causes 1/3 and ½ subharmonic peaks to show up and also significantly increases the amplitude of vibration of the "stalling" rotor. In this case the large vibration amplitudes of the stalling cracked rotor might well exceed the rotor static deflection and therefore violate the common weight dominance assumption made in the study of rotors with breathing cracks.

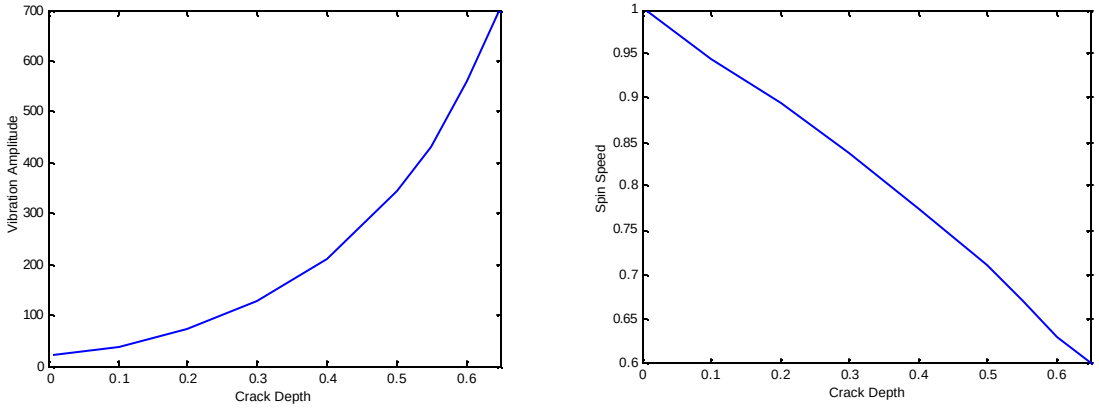

(a) **(b)**

Fig. 5. Normalized spin speed (a) and maximum vibration amplitude (b) as a function of crack depth at the rotor stalling; $T = 0.01$, $(e/r)^2 = 0.85 \times 10^{-3}$, $g/(ew_n^2) = 5$, $V = 0.02$.

For the rotor in stall and under the constant driving torque, its normalized spin speed and vibration amplitude as a function of crack depth is presented in Fig. 5. It can be seen that while the rotor vibration amplitude increases parabolically (Fig. 5(a)) the stalling speed almost linearly decreases with the depth of the crack (Fig. 5(b)).

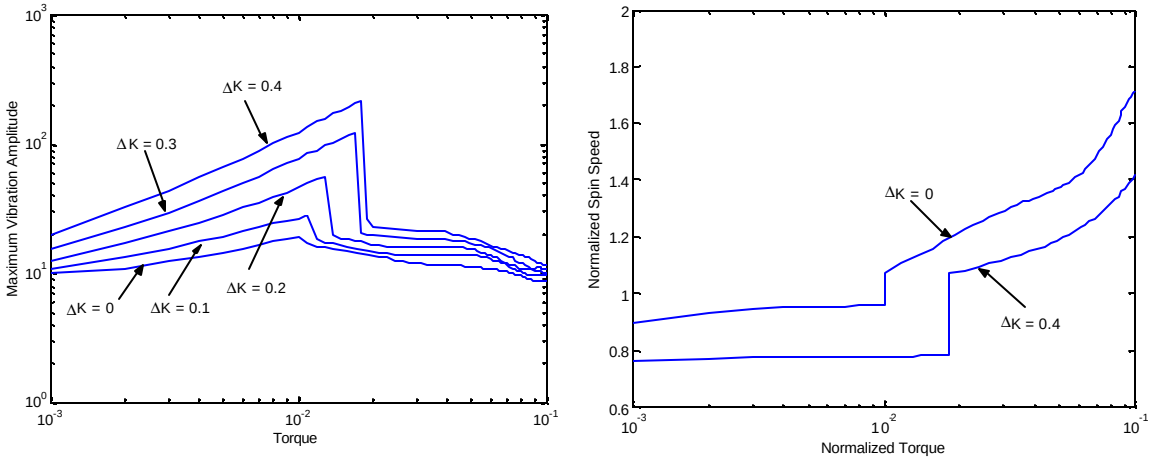

(a) **(b)**

Fig. 6. Maximum normalized vibration amplitude (a) and the corresponding maximum normalized spin speed (b) of the rotor as a function of constant torque for various crack depths; $V = 0.03$, $(e/r)^2 = 0.001$, $g/(ew_n^2) = 5$.

The effect of the applied constant torque and various crack depths on the maximum rotor resonant vibration amplitude and the spin speed for various crack depths is shown in

Fig. 6. The peak of each curve in Fig. 6(a) denotes the threshold value of the constant driving torque below which the rotor is locked in the resonance and above which the rotor is capable to overcome the resonance.

For the range of torques below the threshold value (i.e., in the stalling zone), the rotor maximum vibration amplitude increases for increasing value of torque (Fig. 6(a)) and the corresponding stalling spin speed remains almost constant (Fig. 6(b)), indicating lack of rotor acceleration. Also, in the stalling zone while the maximum vibration amplitude grows with the increased depth of the crack the corresponding rotor stalling speed decreases. Increase of the drive torque accelerates the cracked rotor locked in the resonance zone and at the same time reduces its resonance maximum vibration amplitude and move the resonance peak to higher spin speeds.

5. CONCLUSIONS

The following conclusions can be drawn based on the results presented in this paper:

1. The developed model enables to study the cracked rotor dynamic response with and without weight dominance in the presence of nonsynchronous whirl. The model includes small and deep cracks, as well as cross stiffness effect (for deep cracks).
2. The stalling effect of the rotor is crack sensitive, i.e., even minute increase of crack depth can cause rotor to stall. This is accompanied by the presence of subcritical (1/3, ½) response peaks and large increase of fundamental vibration response.
3. For rotor in stalling zone its maximum vibration amplitude increases for increasing value of torque and the corresponding stalling spin speed remains almost constant.
4. For the stalled rotor the maximum vibration amplitude grows parabollically with the increased depth of the crack and the corresponding rotor stalling speed decreases almost linearly.

REFERENCES

1. Sawicki, J.T., Some Advances in Diagnostics of Rotating Machinery Malfunctions, Invited Paper, *Proc. of International Symposium on Machine Condition Monitoring and Diagnosis*, The Japan Society of Mechanical Engineers, (2002) 138-144.
2. Sekhar, A. S., Prabhu, B. S., Transient Analysis of Cracked Rotor Passing Through Critical Speed, *Journal of Sound and Vibration*, Vol. 173 (3) (1994) 415-421
3. Sekhar, A. S., Prabhu, B. S., Condition Monitoring of Cracked Rotors Through Transient Response, *Mechanism and Machine Theory*, Vol. 33, Issue 8 (1998) 1167-1175.
4. Sawicki, J. T., Wu, X., Baaklini, G.Y. and Gyekenyesi, A., Vibration-Based Crack Diagnosis in Rotating Shafts During Acceleration Through Resonance, *Proceedings of SPIE*, Vol. 5046 (2003).
5. Markert R., Pfützner H. and Gasch R., Biegeschwingungsverhalten rotierenden Wellen beim Durchlaufen der kritischen Drehzahlen, *Konstruktion*, 29 (1977) 355-365.

6. Gasch R, Markert R. and Pfutzner H., Acceleration of Unbalance Flexible Rotors Through the Critical Speeds, *Journal of Sound and Vibration*, 63(3), (1979) 393-409.
7. Genta, G. and Delprete, C., Acceleration Through Critical Speeds of an Anisotropic, Non-Linear, Torsionally Stiff Rotor with Many Degrees of Freedom, *Journal of Sound and Vibration*, 180(3), (1995) 369-386.
8. Wauer, J., On the Dynamics of Cracked Rotors: A Literature Survey, *Applied Mechanics Reviews*, Vol. 43(1) 1990 13-17.
9. Dimarogonas, A. D., Vibration of Cracked Structures: A State of the Art Review, *Engineering Fracture Mechanics*, Vol. 55, No. 5, (1996) 831-857.
10. Gasch, R. A, 1993, Survey of the Dynamic Behavior of a Simple Rotating Shaft with a Transverse Crack. *Journal of Sound and Vibration*, 160(2), (1993) 313-332.
11. Penny, J. E. T. and Friswell,, M.I., Simplified Modelling of Rotor Cracks, *Proc. ISMA 27*, Leuven, Belgium, (2002) 607-615.
12. Mayes, I. W. and Davies, W. G. R., A Method of Calculating the Vibrational Behavior of Coupled Rotating Shafts Containing a Transverse Crack, *Proc. of International Conference on Vibrations in Rotating Machinery*, Paper C254/80, IMechE, (1980) 12-27.
13. Mayes, I. W. and Davies, W. G. R., Analysis of the Response of a Multi-Rotor-bearing System Containing a Transverse Crack in a Rotor, *Journal of Vibration, Acoustics, Stress, and Reliability in Design, Trans. ASME*, Vol. 106, (1984) 139-145.

NOMENCLATURE

C	external damping coefficient
$f(y)$	crack steering function
J_p	moment of inertia of the disk
K	stiffness of uncracked shaft
M	mass of the disk
r	radius of gyration
t, t	time; $t = w_n t$
T_a, T	driving torque; $T = T_a / J_p w_n^2$
z, y, Z, Y	inertial coordinates; $Z = z/e$, $Y = y/e$
a	acceleration ratio
b	angle between crack and unbalance eccentricity
Δk_x	the largest stiffness change ratio in x -direction caused by crack
Δk_h	the largest stiffness change ratio in h -direction caused by crack
ΔK	stiffness change ratio $(= \Delta k_x / K)$
e	eccentricity of the disk
V	external damping ratio
q	angular position of the eccentricity e in the inertial system
x, h	body fixed rotating coordinates, x is in the crack direction
w_n	undamped critical speed of uncracked rotor